

## The discovery of carboline analogs as potent MAPKAP-K2 inhibitors

Jiang-Ping Wu,<sup>\*</sup> Ji Wang, Asitha Abeywardane, Denise Andersen, Michel Emmanuel, Elda Gautschi, Daniel R. Goldberg, Mohammed A. Kashem, Susan Lukas, Wang Mao, Leslie Martin, Tina Morwick, Neil Moss, Christopher Pargellis, Usha R. Patel, Lori Patnaude, Gregory W. Peet, Donna Skow, Roger J. Snow, Yancey Ward, Brian Werneburg and Andre White

*Research and Development, Boehringer-Ingelheim Pharmaceuticals, 900 Ridgebury Road, Ridgefield, CT 06877, USA*

Received 9 April 2007; revised 21 May 2007; accepted 22 May 2007

Available online 7 June 2007

**Abstract**—The discovery of a series of potent, carboline-based MK2 inhibitors is described. These compounds inhibit MK2 with IC<sub>50</sub>s as low as 10 nM, as measured in a DELFIA assay. An X-ray crystal structure reveals that they bind in a region near the p-loop and the hinge region of MK2a.

© 2007 Elsevier Ltd. All rights reserved.

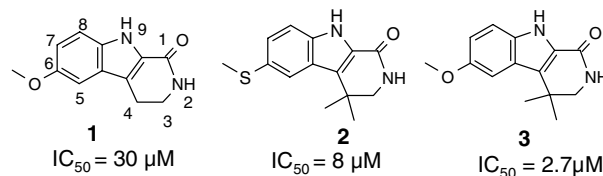
Mitogen activated protein kinases (MAPKs) are signal transduction molecules that control the expression of a variety of gene products involved in inflammation, cell proliferation, and apoptosis.<sup>1</sup> Of the four major classes of MAPKs,<sup>2</sup> the p38 MAPK family activates a wide range of regulatory proteins upon stimulation by external signals. The p38 pathway has long been a drug discovery target for pharmaceutical companies.<sup>3</sup>

MAPKAP-K2 (MK2), a substrate of p38 MAPKs, plays central roles in p38 mediated signal transduction. In mice genetically deficient in MK2, the production of pro-inflammatory cytokines, such as tumor necrosis factor- $\alpha$  (TNF- $\alpha$ ), interleukin-1 $\beta$  (IL-1 $\beta$ ), IL-6, and interferon- $\gamma$  (IFN- $\gamma$ ), is inhibited significantly following stimulation of splenocytes with lipopolysaccharide (LPS). Moreover, this phenotype cannot be rescued by the expression of a kinase dead MK2 mutant, indicating that the kinase function of MK2 is required for pro-inflammatory cytokine production.<sup>4</sup> Thus, inhibitors of MK2 kinase activity are potentially useful for treatment of inflammatory diseases such as toxic shock syndrome, rheumatoid arthritis, osteoarthritis, diabetes, and

inflammatory bowel disease.<sup>5</sup> In fact, a number of pharmaceutical companies have disclosed drug discovery programs targeting this kinase.<sup>6</sup>

Our program to develop small molecule MK2 inhibitors began with high throughput screening that identified two carboline analogs, **1** and **2**, as moderate MK2 inhibitors (Fig. 1).<sup>7</sup> A simple combination of the structural features of **1** and **2** produced a more potent analog **3**. This prompted us to start a chemistry program to further explore this class of compounds. In this paper, we report our SAR studies that led to a series of potent carboline-based MK2 inhibitors.

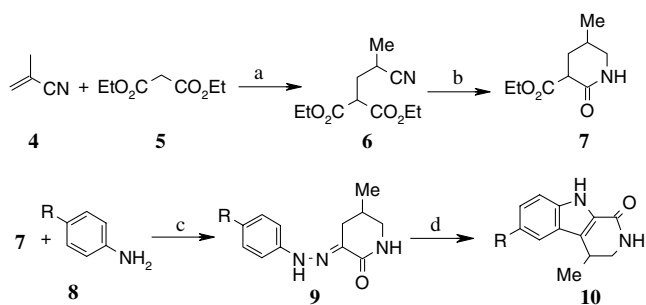
Compounds in Tables 1–6 were prepared according to Schemes 1 and 2. Reaction of methylacrylonitrile (**4**) and diethyl malonate (**5**) under basic conditions provided



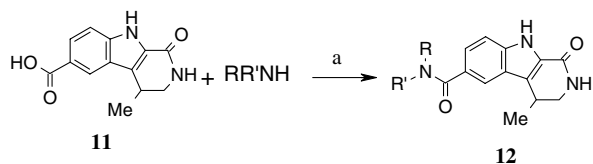
**Keywords:** MAPKAP-K2; MK2; MK2a; Carboline.

<sup>\*</sup> Corresponding author. Tel.: +1 203 798 4982; fax: +1 203 791 6072; e-mail: [jwu@rdg.boehringer-ingelheim.com](mailto:jwu@rdg.boehringer-ingelheim.com)

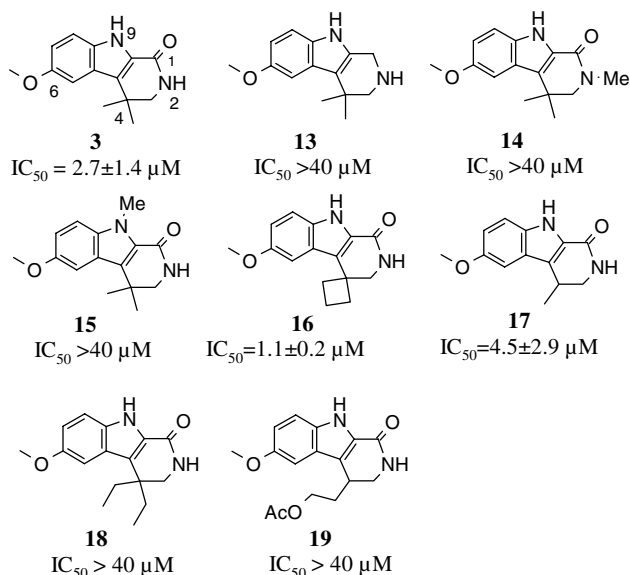
**Figure 1.** MK2 inhibitors discovered via high throughput screening. IC<sub>50</sub>s were obtained in a DELFIA assay.<sup>7</sup>



**Scheme 1.** Reagents and conditions: (a) NaOEt, EtOH, rt, 88%; (b) 1—H<sub>2</sub>, Pt<sub>2</sub>O, EtOH, 2—100 °C, 70–80%; (c) 1—NaNO<sub>2</sub>, HCl, 0–10 °C, 2—KOH, 70–80%; (d) formic acid, reflux, 50–70%.



**Scheme 2.** Reagents and conditions: (a) EDC, HOBT, DMAP (cat.), DMF, rt to 60 °C, overnight 50–90%.



**Figure 2.** Preliminary SAR.

compound **6**. Hydrogenation of compound **6** followed by heating gave a cyclic lactam **7**. Compound **7** was next reacted with a diazonium intermediate derived from aniline **8** to generate hydrazone **9**, which was refluxed in formic acid to provide a carboline analog **10** (Scheme 1).

Amide analogs **12** were prepared via EDC mediated coupling of carboline 6-carboxylic acid **11** and corresponding amines (Scheme 2).

Our initial SAR studies were aimed at identifying structural features exploitable for improving compound potency. Thus, the major functional groups in compound **3** were individually modified (Fig. 2 and

**Table 1.** SAR at 6-position

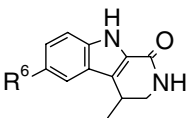
		
Compound	R <sup>6</sup>	IC <sub>50</sub> (μM)
<b>20</b>	H	>40
<b>21</b>	Me	>40
<b>22</b>	Ph	>40
<b>23</b>	Br	15 ± 13
<b>24</b>	HO	>40
<b>17</b>	MeO	4.5 ± 2.9
<b>25</b>	BnO	>40
<b>26</b>	AcNH	>40
<b>27</b>	H <sub>2</sub> N(CO)	5.4 ± 2.9

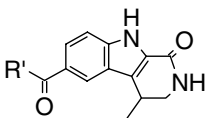
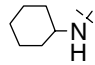
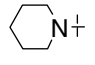
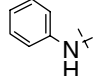
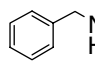
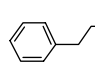
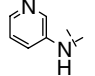
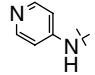
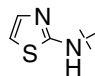
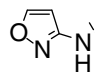
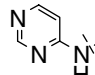
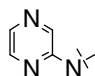
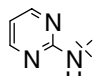
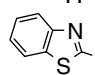
Table 1). Removal of the carbonyl group at C1 diminished potency (**13**). Methylation of either N2 or N9 gave inactive compounds (**14** and **15**). At C4, replacement of the gem-dimethyl group with a cyclobutyl group or removal of one of the methyl groups did not show significant effects (**16** and **17**). However, larger alkyl substituents or substituents containing polar groups were not tolerated (**18** and **19**) (Fig. 2). On the left side of the structure, replacement of the C6-OMe group in compound **17**<sup>8</sup> with H, Ph, Me, OH or AcNH abolished activity (**20–26**). The larger benzyl ether analog **25** was also inactive. The only C6-OMe replacement tolerated was an amide group: compound **27** displayed potency comparable to that of compound **17** (Table 1).

The C6 amide moiety in **27** was further derivatized. A series of aliphatic and aromatic amides were synthesized (Table 2). Aliphatic amides were not active (**29–31**, **33**, and **34**), the only exception being the methyl amide **28**, which was weakly active (IC<sub>50</sub> = 12 μM). On the other hand, aromatic or heteroaromatic amides mostly displayed better potency compared to the unsubstituted amide **27** (**32** and **35–42**). Among the more potent analogs were pyridyl amides **35**, **36** and thiazole amide **37**, showing IC<sub>50</sub> values below 1 μM.

Following up on these findings, we next examined the effects of substitution on the aromatic amides. A series of substituted phenyl amides were initially synthesized (Table 3). Substitutions at C2' were not tolerated (**43–47**). At C3', large groups reduced potency (**49** and **50**), while smaller substitutions had no significant effect (**51–53** and **55–57**). An exception was the 3'-CN group, which lowered the IC<sub>50</sub> to 770 nM (**54**). At C4', most substitutions showed no significant effects (**58–64** and **66**). However, amide and ester groups at this position improved compound potency moderately (**65**, **67**, IC<sub>50</sub> < 1 μM).

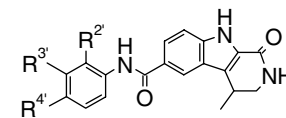
Encouraged by the beneficial effects of amide and ester groups, we next incorporated these groups onto pyridyl and thiazole amides **35** and **37**. As shown in Table 4, neither ester nor amide moiety improved the potency of pyridyl amide **35** (**68** and **69**). However, an amide substitution increased the potency of thiazole analog **37** significantly: compounds **71** and **73** gave IC<sub>50</sub> values of 83 and 120 nM, respectively.

**Table 2.** C6-amide analogs

		
Compound	R'	IC <sub>50</sub> (μM)
27	H <sub>2</sub> N	5.4 ± 2.9
28	MeHN	12 ± 1
29	Me <sub>2</sub> N	>20
30		>20
31		>20
32		2.9 ± 0.1
33		>20
34		>20
35		0.52 ± 0.15
36		0.76 ± 0.17
37		0.82 ± 0.26
38		1.50 (n = 1)
39		1.50 ± 0.14
40		0.44 ± 0.11
41		>20
42		1.5 ± 0.8

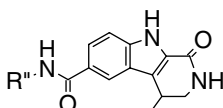
Further derivatization of the thiazole amides followed (Table 5). For analogs of **71**, addition of one methyl group to the amide nitrogen gave a compound of similar potency (**74**). However, dimethylation of the

**Table 3.** Effects of substitution on phenyl amide

				
Compound	R <sup>2'</sup>	R <sup>3'</sup>	R <sup>4'</sup>	IC <sub>50</sub> (μM)
32	H	H	H	2.9 ± 0.1
43	Me	H	H	>20
44	F	H	H	9.7 ± 1.9
45	Br	H	H	>10
46	CN	H	H	>10
47	CONH <sub>2</sub>	H	H	3.0 (n = 1)
48	H	Me	H	3.4
49	H	<i>i</i> -Pr	H	>20
50	H	<i>t</i> -Bu	H	>20
51	H	F	H	1.7 (n = 1)
52	H	Cl	H	1.3 ± 0.4
53	H	Br	H	2.7 (n = 1)
54	H	CN	H	0.77 ± 0.57
55	H	CO <sub>2</sub> Et	H	7.4 ± 0.2
56	H	AcNH	H	4.4 (n = 1)
57	H	CONH <sub>2</sub>	H	2.7 (n = 1)
58	H	H	Me	3.0 ± 0.7
59	H	H	<i>i</i> -Pr	7.7 ± 0.2
60	H	H	<i>t</i> -Bu	>20
61	H	H	F	3.0 (n = 1)
62	H	H	Cl	1.7 ± 0.6
63	H	H	Br	7.0 (n = 1)
64	H	H	CN	1.7 ± 0.5
65	H	H	CO <sub>2</sub> Me	0.93 ± 0.02
66	H	H	AcNH	1.8 (n = 1)
67	H	H	CONH <sub>2</sub>	0.62 ± 0.13

amide nitrogen lowered potency a few fold (**75**), suggesting that one of the amide N–H might be engaged in a binding interaction with MK2. Several analogs containing polar groups were also prepared, leading to compounds with improved potency (**76–81**, IC<sub>50</sub> ~ 20–30 nM). Larger lipophilic groups, such as cyclohexyl group in **83**, also had beneficial effect. Incorporation of an *N*-methyl amino group into the 6-membered ring further improved potency, providing compound **85** with an IC<sub>50</sub> of 10 nM. Note that compound **84**, which contains a polar group *and* a 6-membered moiety but lacks an amide N–H, was less active than the parent compound **71**, again demonstrating the importance of the amide N–H. Similar modifications to compound **73** did not show beneficial effects. In fact, substitution of the amides with polar groups reduced activity (**86** and **87**).

An X-ray crystal structure of MK2a—compound **76** complex was obtained (2.9 Å resolution, Fig. 3).<sup>9</sup> The structure revealed that compound **76** binds between the p-loop and residues V118, T206, L193, and Y194 (all not shown), and interacts with the hinge region M138–D142. The oxygen atom of the internal carbonyl amide (at C6) is in close proximity to the NH of L141 (2.6 Å) for H-bonding. The thiazole aryl is nearly co-planar with the carboline scaffold, with

**Table 4.** Substituted pyridyl and thiazole amides


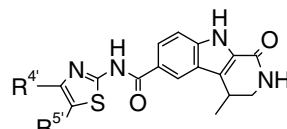
The chemical structure shows a carboline core (a benzene ring fused to a pyrrole ring). An amide group (-C(=O)NH-) is attached to the benzene ring at the 4-position. The nitrogen of this amide is substituted with an R'' group. The pyrrole ring has a methyl group at the 2-position and a carbonyl group at the 3-position.

Compound	R''	IC <sub>50</sub> (μM)
35		0.52 ± 0.15
68		0.76 ± 0.13
69		0.62 ± 0.27
37		0.82 ± 0.26
70		0.75 (n = 1)
71		0.083 ± 0.028
72		0.77 ± 0.33
73		0.12 ± 0.01

dihedral angle of ~17°. The external amide (at 4' of thiazole moiety) is nearly co-planar to the thiazole ring and presents its NH proton inward, forming a second H-bond with L70 (3.1 Å). However, the portion beyond the external amide bond, which apparently contributes to compound potency, is not shown to engage in binding interactions. Additionally, the carboline amide oxygen [C1=O] and nitrogen (N2), shown by SAR to be essential for compound potency, are not within bonding distances to nearby amino acid residues or peptide backbones.

Selected compounds were tested for cellular activity and kinase selectivity (Table 6). In an assay that measures LPS-stimulated TNF-α production from THP-1 cells,<sup>10</sup> the majority of these compounds did not show measurable activity (IC<sub>50</sub> > 10 μM). Compound **83**, an analog without a terminal polar group, was among the few that were active in the assay.<sup>11</sup> In the MK1 and ERK2 kinase assays,<sup>12,13</sup> these compounds showed moderate activity (IC<sub>50</sub> ~ 1 μM). Improving cellular activity and kinase selectivity thus became the focus of our subsequent chemistry efforts, which will be reported in future publications.

In conclusion, we have discovered a series of potent carboline-based MK2 inhibitors. In a DELFIA, the most active compounds inhibit MK2 with IC<sub>50</sub> values

**Table 5.** Substituted thiazole amides


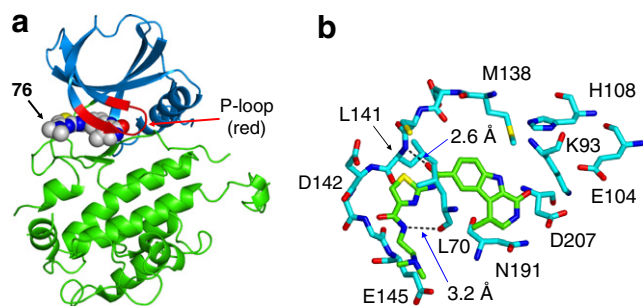
The chemical structure shows a carboline core. An amide group (-C(=O)NH-) is attached to the benzene ring at the 4-position. The nitrogen of this amide is substituted with a thiazole ring. The thiazole ring has substituents R<sup>4'</sup> and R<sup>5'</sup> at the 2 and 5 positions, respectively.

Compound	R <sup>4'</sup>	R <sup>5'</sup>	IC <sub>50</sub> (μM)
71	NH <sub>2</sub> (CO)-	H	0.089 ± 0.027
74	MeNH(CO)-	H	0.072 ± 0.014
75	Me <sub>2</sub> NC(O)-	H	0.333 ± 0.085
76	Me <sub>2</sub> N(CH <sub>2</sub> ) <sub>2</sub> NHC(O)-	H	0.034 ± 0.014
77	H <sub>2</sub> N(CH <sub>2</sub> ) <sub>2</sub> NHC(O)-	H	0.017 ± 0.002
78	Me <sub>2</sub> N(CH <sub>2</sub> ) <sub>3</sub> NHC(O)-	H	0.035 ± 0.010
79	H <sub>2</sub> N(CO)CH <sub>2</sub> NHC(O)-	H	0.124 ± 0.054
80	H <sub>2</sub> N(CO)(CH <sub>2</sub> ) <sub>2</sub> NHC(O)-	H	0.021 ± 0.009
81	HO(CH <sub>2</sub> ) <sub>2</sub> NHC(O)-	H	0.031 (n = 1)
82	Me(CH <sub>2</sub> ) <sub>2</sub> NHC(O)-	H	0.045 ± 0.018
83		H	0.044 ± 0.004
84		H	0.25 ± 0.10
85		H	0.010 ± 0.001
73	H	H <sub>2</sub> NC(O)-	0.13 ± 0.02
86	H	Me <sub>2</sub> N(CH <sub>2</sub> ) <sub>2</sub> NHC(O)-	1.3 (n = 1)
87	H	Me <sub>2</sub> N(CH <sub>2</sub> ) <sub>3</sub> NHC(O)-	0.48 ± 0.07

**Table 6.** Selectivity and cellular activities

Compound	MK2 IC <sub>50</sub> (μM)	MK1 IC <sub>50</sub> (μM)	ERK2 IC <sub>50</sub> (μM)	THP-1 IC <sub>50</sub> (μM)
71	0.089 ± 0.027	0.75 ± 0.01	0.56 ± 0.15	>5
76	0.034 ± 0.014	0.66 ± 0.14	1.9 ± 0.0	>5
78	0.017 ± 0.002	—	1.3 ± 0.1	>5
79	0.035 ± 0.010	0.80 ± 0.21	1.5 ± 0.4	>5
83	0.044 ± 0.004	—	—	1.60 ± 0.00
85	0.011 ± 0.001	—	—	>5
35	0.52 ± 0.15	1.2 ± 0.9	0.21 ± 0.06	>5

in the low nanomolar range. A crystal structure revealed that this compound class binds between p-loop and residues V118, T206, L193, and Y194, and interact with the hinge region of MK2a (M138–D142). These compounds are moderately selective against MK1 and ERK2. However, most of these analogs are not active in a cellular (THP-1) assay.



**Figure 3.** X-ray structure of MK2a [41–364] co-crystallized with compound **76**.

### Supplementary data

Experimental procedures for crystal complex formation and X-ray data collection; synthetic schemes for compounds in Figure 2. This material is available free of charge via internet. Supplementary data associated with this article can be found, in the online version, at doi:10.1016/j.bmcl.2007.05.101.

### References and notes

- Robinson, M. J.; Cobb, M. H. *Curr. Opin. Cell Biol.* **1997**, 9, 180.
- There are four major families of MAPKs: (1) the archetypal extracellular regulated kinases (ERKs), (2) the c-jun N-terminal kinases (JNKs), (3) the p38 MAPKs, and (4) the ERK5 or BigMAPKs, see: Tibbles, L. A.; Woodgett, J. R. *Cell. Mol. Life Sci.* **1999**, 55, 1230.
- (a) Jackson, P. F.; Bullington, J. L. *Curr. Topics Med. Chem.* **2002**, 2, 1009; (b) Cirillo, P. F.; Pargellis, C. A.; Regan, J. *Curr. Top. Med. Chem.* **2002**, 2, 1021, and references cited therein.
- Kotlyarov, A.; Yannoni, Y.; Fritz, S.; Laaß, K.; Telliez, J.-B.; Pitman, D.; Lin, L.-L.; Gaestel, M. *Mol. Cell. Biol.* **2002**, 22, 4827.
- Dinarello, C. A. *Nutrition* **1995**, 11, 492; *Rev. Infect. Dis.* **1984**, 6, 51; *Curr. Opin. Pharmacol.* **2004**, 4, 378.
- (a) A selection of patent and patent applications claiming MK2 inhibitors is listed below Meyers, M. et al. WO2005009370, US20050143371, US20050137220, US 20050101623; (b) Anderson, D. R. et al. WO2004055015; WO2004054505; WO2004054504; US2004127519, US2004 127511, US2004 142978; (c) Vazquez, M. L. et al. US20 04127492; (d) Buzon, R. A. et al. WO2004020440; WO 2004020438; (e) Sato, H. et al. WO2005007092; (f) Kataoka, K. et al. WO2004076458; (g) Aronov, A. et al. WO2004037814; (h) Hodge, C. N. et al. WO2005/033102; (i) Wyatt, P. et al. WO2005014554
- A dissociation-enhanced lanthanide fluorescent immunoassay (DELFA) of MK2 catalysis was employed to determine the potency of MK2 inhibition, see: (a) Lukas, S. M.; Kroe, R.; Wildeson, J.; Peet, G. W.; Frego, L.; Davidson, W.; Ingraham, R. H.; Pargellis, C. A.; Labadia, M. E.; Werneburg, B. G. *Biochemistry* **2004**, 43, 9950; (b) *Assay protocol*: The GST-MK2a 1–400 variant of MK2 was activated with p38 $\alpha$  MAPK by methods similar to those described previously<sup>7</sup> and re-purified by GSH affinity chromatography. The GST-LSP1 179–339 substrate of MK2 was biotinylated with a 70-fold molar excess of PEO-iodoacetyl biotin (Pierce), followed by quenching with excess DTT and purification by Sephadex G-25 gel filtration. A mouse monoclonal anti-phospho-LSP1 IgG1 antibody was generated to mcKLH (Pierce) conjugated phospho-peptide antigen, CRTPKLARQA-pS-IELPSM, from AnaSpec. The anti-phospho LSP1 IgG1 antibody was labeled with the Eu-chelate of *N*<sup>1</sup>-(*p*-isothiocyanatobenzyl)-diethylenetriamine-*N*<sup>1</sup>,*N*<sup>2</sup>,*N*<sup>3</sup>,*N*<sup>3</sup>-tetraacetic acid (Perkin Elmer Life Sciences) for the DELFIA of MK2 catalysis and inhibition. Compounds and activated GST-MK2a 1–400 (1 nM) were incubated in neutravidin coated plates (Pierce) at 25 °C in the following 40  $\mu$ L reaction mixture for 30 min: 50 mM HEPES (pH 7.6), 50 mM KCl, 10 mM MgCl<sub>2</sub>, 100  $\mu$ M Na<sub>3</sub>VO<sub>4</sub>, 0.01% CHAPS, 1 mM DTT, 10  $\mu$ g/mL bovine serum albumin, 1% DMSO, 500 nM biotinylated GST-LSP1 179–339, and 2  $\mu$ M ATP. The plates were washed with 25 mM Tris–HCl (pH 7.5), 150 mM NaCl, and 0.05% Tween 20. Eu-chelated anti-phospho-LSP1 IgG1 antibody (0.5 mg/mL) was diluted 1:20,000 in 50 mM Tris–HCl (pH 7.5), 150 mM NaCl, 10  $\mu$ M DTPA, 0.05% Tween 40, 0.2% bovine serum albumin, and 0.05% BGG; 40  $\mu$ L of the diluted antibody solution was added to the plates. After 1-h incubation at 25 °C, the plate was washed prior to the addition of DELFIA enhancement solution (Wallac #4001-0010), and read after 15 min at ex  $\lambda$  = 360 nm and em  $\lambda$  = 620 nm.
- The synthesis of the C4-monomethyl analog **17** is considerably easier than that of C4-gem-dimethyl analog **3**. Since compounds **17** and **3** are comparable in potency, we chose compound **17** as the reference compound for initial SAR studies. Later studies (to be published in separate papers) showed that in more advanced structures, the C4-gem-dimethyl moiety improved potency moderately.
- (a) The X-ray coordinates have been deposited with RCSB Protein Data Bank, deposition #2PZY; The protein used in this study is a segment of MK2a containing residues 41–364. For a detailed crystal structure of a different MK2 complex, in which MK2 is bound to its activator p38, see: (b) White, A.; Pargellis, C. A.; Studts, J. M.; Werneburg, B. G.; Farmer, B. T., II *Proc. Natl. Acad. Sci. U.S.A.* **2007**, 104, 6353.
- For the THP-1 assay protocol, see: Regan, J.; Breitfelder, S.; Cirillo, P.; Gilmore, T.; Graham, A. G.; Hickey, E.; Klaus, B.; Madwed, J.; Moriak, M.; Moss, N.; Pargellis, C.; Pav, S.; Proto, A.; Swinamer, A.; Tong, L.; Torcellini, C. *J. Med. Chem.* **2002**, 45, 2994.
- It is conceivable that poor membrane permeability contributed to the lack of cellular potency for compounds with terminal polar groups. This was investigated subsequently, the results of which will be published separately.
- The selectivity against MK1a and ERK2 was determined in an IMAP assay, see: (a) Sportsman, J.; Daijo, J.; Gaudet, E. A. *Comb. Chem. High Throughput Screening* **2003**, 6, 195; (b) *Assay protocol*: Compounds were diluted with DMSO in kinase assay buffer (10 mM Tris–HCl (pH 7.2), 10 mM MgCl<sub>2</sub>, 0.01% Tween 20, and 1 mM DTT) such that the final concentration of DMSO was 1%. The diluted compounds were incubated with kinase, ATP and peptide substrate in Corning 96-well half-area, black non-binding surface microtiter plates in kinase assay buffer for 90 min at room temperature. The MK1a reaction consisted of 250 pM MK1a (Upstate Catalog #14-509), 1  $\mu$ M ATP, and 100 nM FAM-S6 ribosomal protein-derived peptide. The ERK2 reaction consisted of 100 pM ERK2 (Upstate Catalog #14-173), 2.5  $\mu$ M ATP, and 100 nM FAM-Erktide. The kinase reactions were halted by addition of IMAP progressive binding reagent in each well. After 30 min of incubation at room temperature, the plates were read for fluorescence polarization on an

Analyst Plate Reader using  $\text{ex}\lambda = 485\text{ nm}$ ,  $\text{em}\lambda = 530\text{ nm}$ , and FL 505 dichroic mirror.

13. MK1 and ERK2 were selected as primary targets for kinase selectivity testing. This was mainly due

to our desire to avoid inhibiting kinases involved in growth differentiation. The close homology of MK1 to MK2 was another reason for screening against this kinase.